WIND TUNNEL TESTS OF A SLOTTED FLAPPED WING SECTION FOR VARIABLE GEOMETRY SAILPLANES

by D. J. Marsden and R. W. Toogood

Department of Mechanical Engineering
University of Alberta

Abstract

A Variable Geometry Sailplane uses a large full span retractable flap to extend the operating flight speed range from slow flight needed for climb to high speed flight for cruise. The slotted flap wing section has advantages over the earlier chord extending type flap in that it is simpler mechanically and is better able to accommodate strong aileron control. A new slotted flap wing section designed at the University of Alberta has been tested in the low speed wind tunnel. It shows lift characteristics that will be suitable for a variable geometry sailplane, with particularly docile stall characteristics for safe handling.

The extent of laminar flow on this wing section was stabilized by the use of laminar separation bubbles as a mechanism for transition. It was found experimentally that additional drag caused by these laminar separations could be reduced by the introduction of boundary layer trips just ahead of the laminar bubbles. These were effective in reducing the drag even when they were not big enough to trip the boundary layer to cause transition. Overall performance of this wing section was comparable to the FX67-VC-170/1.36 designed by Professor Wortmann for the Sigma project.

Introduction

Mechanisms to alter wing geometry in flight are common to all aircraft in the form of control devices such as ailerons and flap systems. As applied to Sailplanes, Variable Geometry implies large flaps which produce an increase in the effective wing area, or mechanically variable span, or mechanically variable wing thickness. The objective is much the same as for other aircraft using flaps, to provide a better compromise between requirements of low drag for cruising flight, and high lift for low speed flight. In the case of the sailplane there is an additional requirement that high lift be produced with the minimum possible drag for climbing flight in thermals where it is important to maintain a low sink rate.

Two types of flap systems have been used for variable geometry sailplanes. The first is the chord extending non-slotted Fowler flap used on the British Sigma[1] and more recently the SB-11[2] and Mu 25 aircraft produced by West German Akaflieg groups. The advantage claimed for this type of flap system is low wing profile drag in the flap extended configuration. Disadvantages, which showed up on the Sigma Project, are difficulties with accommodating a large chord extending flap within the wing, and with integration of suitably effective control mechanisms into such a flap system.

The second type of flap system is the slotted Fowler flap or slotted flap. Fowler flaps were used on the BJ series of aircraft in South Africa[3] and a more limited motion slotted flap system on the Gemini[4] in Canada. The Sigma prototype has also been refitted with a slotted flap system of the type used on Gemini and this was flight tested in Canada. The main advantages of the slotted flap system as used on Gemini are that flap extension mechanisms are relatively simple and easily fitted into the wing, and that aileron and landing approach control functions can be more easily integrated into the flap system. Aileron control at low speed is particularly effective with part of the slotted flap acting as aileron.

A study of sailplane aerodynamics in circling flight[5] shows that the inducted drag is the major component of overall sailplane drag and that moderately high values of wing profile drag would have relatively little effect on performance. In practice slotted flap wing sections can be designed to have profile drag coefficient very nearly the same as unslotted Fowler flap wing sections.

The variable geometry wing section is really a pair of wing sections. The flap retracted section should have the minimum possible drag at cruising lift coefficient of $0.2 \leq C_L \leq 0.8$. The flap extended low speed wing section should produce an operating lift coefficient of about $C_L = 2$ with the minimum possible profile drag at that lift coefficient. An additional requirement is that there should be some reserve above the operating lift coefficient to avoid loss of control when flying in rough

TABLE 1 Airfoil Coordinates for UA 79-SF-187 Two Element Section

Main Section Coordinates

X	Y-upper	Y-lower
-0.0	-0.0	-0.0
0.0024	0.0056	-0.0034
0.0095	0.0158	-0.0089
0.0212	0.0279	-0.0147
0.0375	0.0400	-0.0205
0.0581	0.0524	-0.0263
0.0828	0.0644	-0.0318
0.1112	0.0760	-0.0371
0.1431	0.0868	-0.0419
0.1781	0.0967	-0.0462
0.2158	0.1055	-0.0499
0.2556	0.1129	-0.0530
0.2973	0.1191	-0.0553
0.3402	0.1239	-0.0571
0.3839	0.1274	-0.0581
0.4278	0.1293	-0.0584
0.4715	0.1299	-0.0577
0.5145	0.1289	-0.0561
0.5561	0.1265	-0.0534
0.5960	0.1229	-0.0495
0.6336	0.1171	-0.0424
0.6686	0.1105	-
0.7005	0.1016	-
0.7290	0.0924	-
0.7536	0.0829	-
0.7742	0.0750	-
0.7905	0.0685	-
0.8023	0.0639	-
0.8094	0.0612	-
0.8117	0.0603	-

Flap Coordinates

X	Y-upper	Y-lower
0.0	-0.0184	-0.0184
0.0048	0.0072	-0.0298
0.0151	0.0264	-0.0341
0.0323	0.0424	-0.0329
0.0472	0.0508	-0.0311
0.0669	0.0578	-0.0281
0.0807	0.0611	-0.0257
0.0976	0.0634	-0.0234
0.1160	0.0644	-0.0208
0.1308	0.0636	-0.0183
0.1458	0.0618	-0.0165
0.1617	0.0584	-0.0137
0.2035	0.0450	-0.0079
0.2409	0.0333	-0.0033
0.2734	0.0230	-0.0003
0.3005	0.0150	0.0006
0.3219	0.0085	0.0009
0.3375	0.0037	0.0007
0.3469	0.0010	0.0003
0.3500	-0.0000	-0.0000

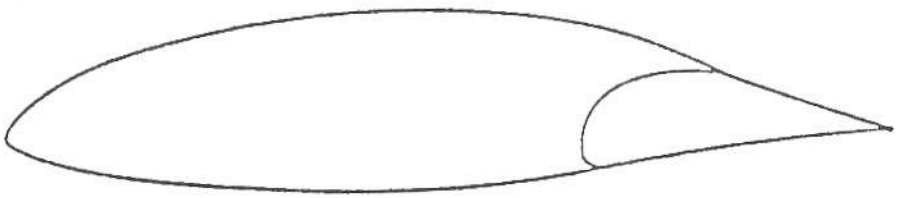

Figure 1. UA79-SF-187 Wing Section

air. In practice this means a maximum lift coefficient of about $C_{Lmax}=2.4$ or 20% above optimum.

A new wing section was designed using the vortex panel iterative design method described in reference 6. A model of this new wing section was tested in the University of Alberta Low Speed Wind Tunnel at Reynolds numbers representative of full scale for a sailplane.

New Wing Section

The flap retracted single element wing section was designed first, followed by design of the flap in the flap extended configuration, keeping the shape of the main part of the wing section constant. In practice, it may be possible to go back and make some changes to the main wing section. For example, changes to the nose shape that are important at high lift with the flap extended are not very critical in the low C_L cruising flight regime.

With the main section shape fixed, the forward upper surface of the flap can be designed in conjunction with the slot shape to give a regular, non-peaky velocity distribution on the flap. The pressure distribution on the flap has a roof top shape followed by a Stratford pressure recovery. The fact that velocity distribution on the flap changes very little with overall wing angles of attack makes it easy to optimize this upper surface velocity distribution.

A flap chord of 35% was chosen arbitrarily as about the largest practical size considering that room must be allowed in the wing for structure and mechanisms. A larger flap chord provides higher Reynolds number for the flap elements and more effective area for the control functions of aileron and landing approach control flap.

A thick wing section was used mainly for structural considerations in that a high aspect radio (about 30:1) will be required for the variable geometry sailplane application. The thick wing section also helps provide a better compromise between high lift and high speed requirements. The shape of the new wing section is shown in **Figure 1**. Wing section coordinates are given in Table 1. This wing section has been given the designation UA79-SF-187 meaning: University of Alberta, 1979, slotted flap, 18.7% thickness chord ratio.

Wind Tunnel Tests

The two dimensional one meter chord model was mounted spanning the short dimension of the 1.22 m × 2.44 m University of Alberta Low Speed Wind Tunnel. Measured turbulence intensity level is 0.1% in this wind tunnel.

Boundary layer control suction was applied through holes drilled in the end plates following the rear 50% of the model contour to eliminate the effect of weak wing tip vortices forming in the tunnel wall boundary layers. For a given angle of attack, measured lift coefficient increased with increasing suction and then stabilized at a constant value for continued increase in suction volume flow. Only quite small amounts of suction were required to reach this stable condition. Flow visualization indicated that the flow was two dimensional. Such features as separation and reattachment lines extended in straight spanwise lines over the entire span outside the tunnel wall boundary layers.

Standard linearized corrections [7] for wall constraint and blockage were applied to measured results.

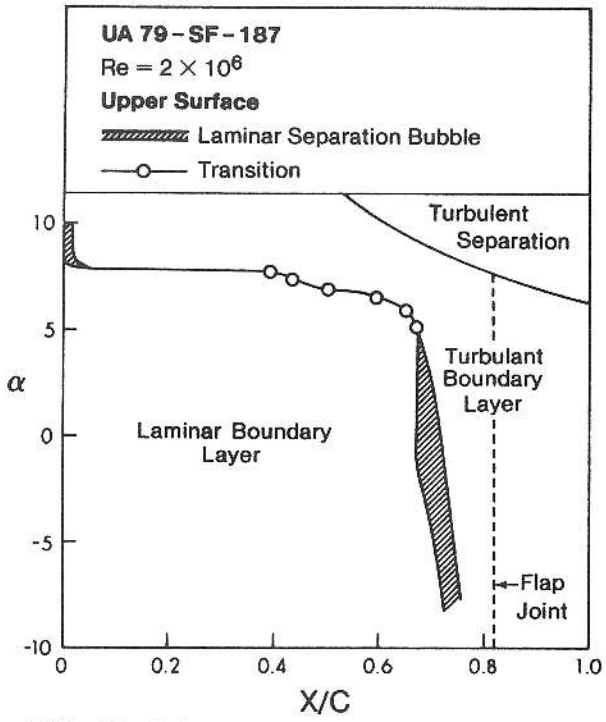

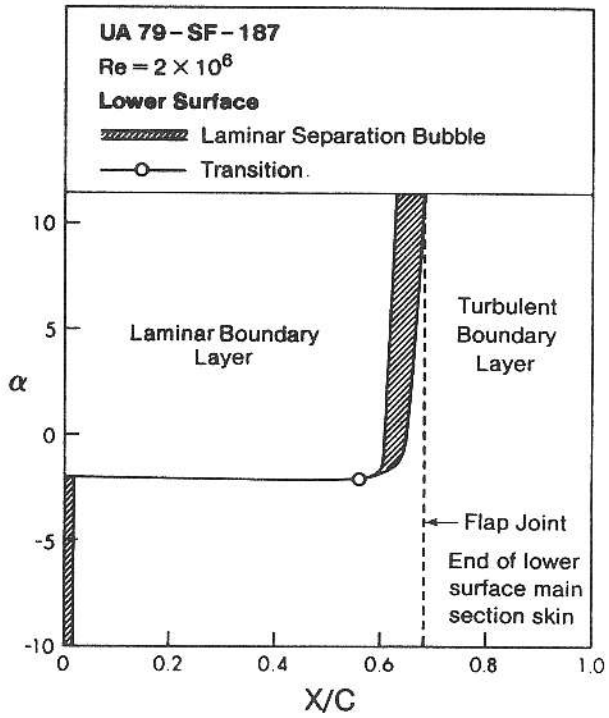

Figure 2. Flow Visualation—Flap Retracted

Model

The 1.0 meter chord model had a 0.5 mm thick aircraft alloy aluminum skin formed over a wood and styrofoam frame. The surface was contoured to shape using automotive body fill, and painted flat black to aid in flow visualization. The contour was accurate to within approximately 1.0 mm (0.1% chord). Fifty-three static pressure taps were provided on the surface to measure pressure distributions. Special care was taken to provide taps very close to the trailing edge of the flap.

Testing Technique

Pressure distributions were measured using a Scanivalve and a single pressure transducer. A data acquisition system incorporating a small computer was used to make pressure measurements, reduce the data to coefficient form and integrate the pressure over the model surface to provide values of lift and pitching moment coefficients.

Drag was measured by means of a pitot traverse through the wake at a point approximately one chord length downstream from the model. Again the data acquisition system was used to make measurements and integrate to provide a direct evaluation of drag coefficient.

Flow visualization was carried out using a type of oil film technique. A mixture of varsol and china clay was painted onto the black surface of the model. This mixture is transparent when wet and turns white when the varsol evaporates leaving behind the china clay residue. Areas with high surface shear stress, as for example in the turbulent boundary layer, dry quickly and turn white. Separation lines show up dark as liquid is deposited there, and reattachment of a laminar separation bubble shows up clearly because the flow splits into a highly turbulent downstream component and a much more slowly moving upstream recirculating component. The presence of the film does not appear to affect the position of transition or separation which is being determined by this technique.

Flow Visualization Results

Results of flow visualization tests are summarized in **Figures 2** and **3** with flap retracted and flap extended respectively ($\delta_f = 20°$). These results show extensive regions of laminar boundary layers, as intended by the choice of velocity distributions in the design. Transition is by means of mid-chord laminar separation bubbles over most of the operating range of this wing section. This behavior is typical of laminar wing sections operating in this Reynolds number regime of 0.5×10^6 to 3×10^6.

Note in Figure 3, that boundary layer flow on the flap is fully attached (except for a small laminar bubble at transition) over the entire range of angles of attack until large scale flow separations occur on the main wing section. This ensures aileron control well into the stall, and a stall warning in the form of buffeting from separations on the main wing section.

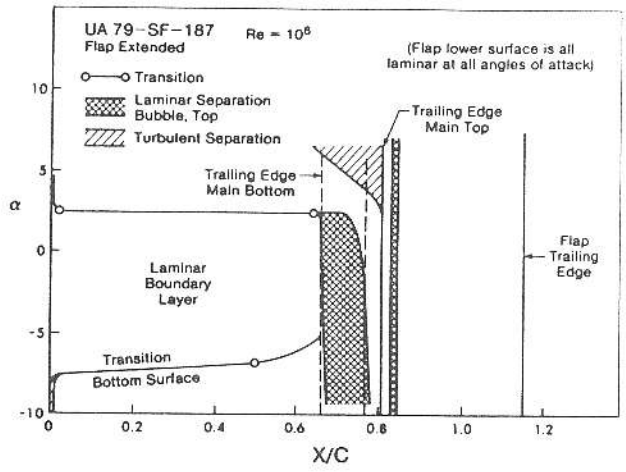

Figure 3. Flow Visualization Results—Flap Extended

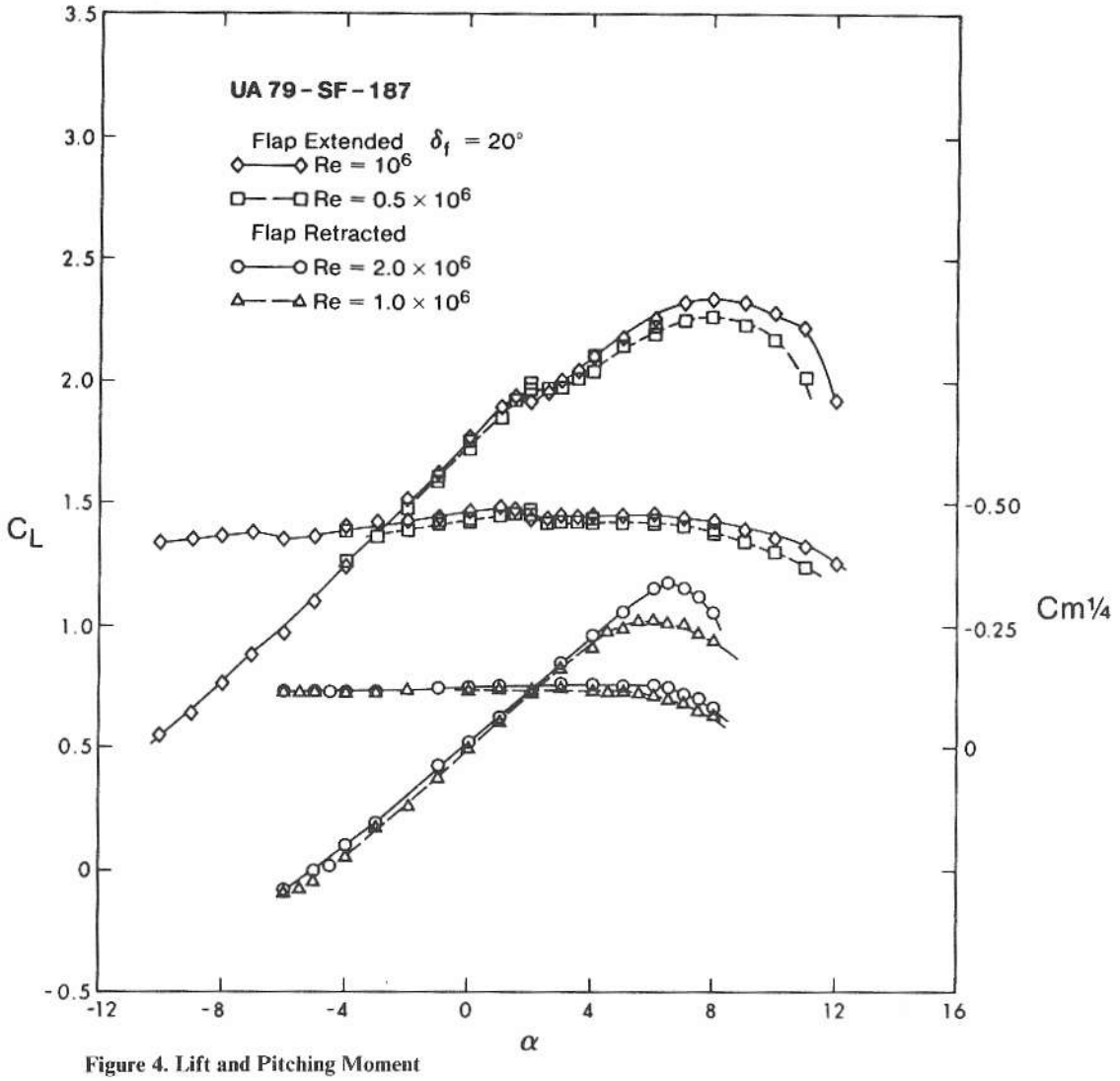

Figure 4. Lift and Pitching Moment

Force and Moment Coefficients

Measured values of lift and moment coefficients as a function of angle of attack are shown in **Figure 4** for the flap retracted and for the flap extended. The flap extended design position was at a deflection of $\delta_f = 20°$, with a gap of 3% chord between the main section upper surface trailing edge and the flap upper surface, and the flap nose 2% chord ahead (overlay) of the main upper trailing edge. The drag characteristics as a function of lift coefficient are shown in **Figure 5**.

Mid-chord laminar bubbles occurring over most of the operating range of this wing section were thought to be contributing significant amounts of drag. The pronounced decrease in drag at high lift both flap retracted and flap extended is due to elimination of the laminar bubble on the upper surface when the adverse pressure gradient over the forward portion of the wing section causes natural transition to occur ahead of the position of the bubble. This transition then quickly moves forward with a further increase in angle of attack resulting in a large increase in drag coefficient.

Some tests were performed to determine the optimum flap extended position. Gaps ranged from 1.7% to 5.7% and overlap ranged from 0 to 4%. Results showed that the section performance was not drastically affected by moving the flap from the design position noted above: there is not a strongly defined optimum point either for lift or drag.

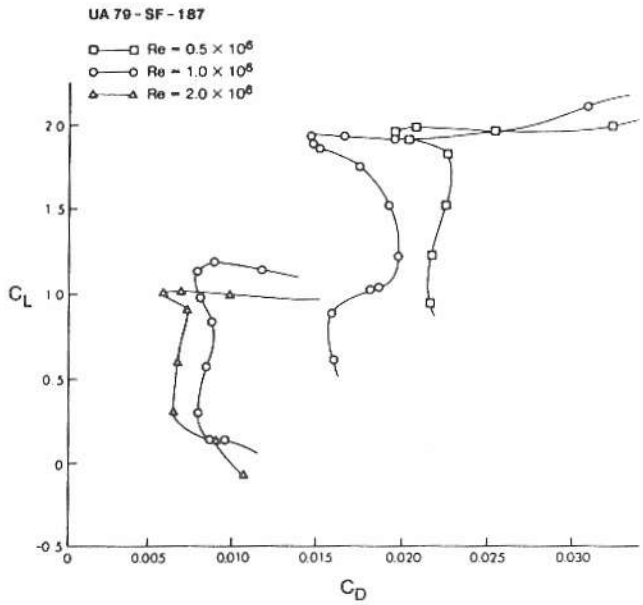

Figure 5. Measured Drag Coefficients

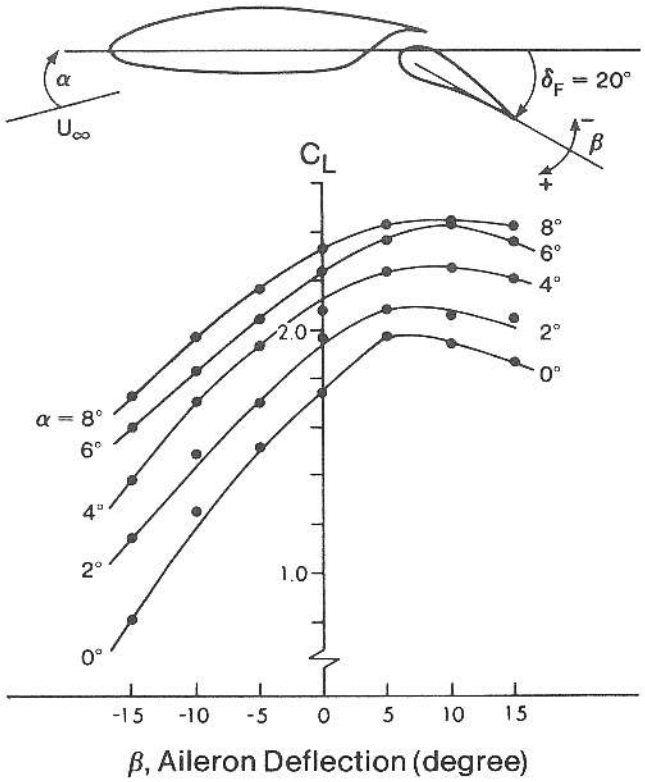

Figure 6. Performance of the Flap as an Aileron

The performance of the flap as an aileron is shown in **Figure 6**. The range of conditions tested corresponded to low speed flight, such as landing or circling in thermals. In these cases, effective aileron control is essential. The flap was hinged at approximately 35% of flap chord for these tests. Figure 6 shows that the section exhibits a mild stall as the aileron deflection increases beyond 5 degrees. The aileron remains effective to high angle of attack ($\alpha = 8°$ corresponds to stall of the main section). As a measure of the aileron effectiveness, $dC_L/d\beta$ has a value 0.045 per degree for normal operations near $C_L = 1.8$.

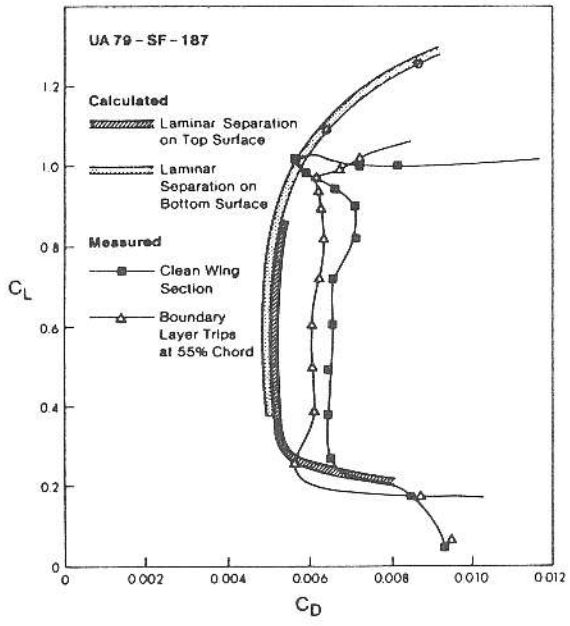

Figure 7. Comparison of Measured and Calculated Drag Coefficient

Laminar Bubble Transition

Laminar separation bubbles provide a mechanism for transition from laminar to turbulent boundary layer flow on most laminar wing sections at Reynolds numbers below about 3×10^6. This wing section was intentionally designed to have a laminar bubble separation which stabilizes transition at 65% chord over the operating range $0.3 < C_L < 1.1$, resulting in nearly constant C_D over this range of lift coefficient.

Figure 7 shows a comparison of measured drag coefficient with that calculated assuming natural transition at the position of predicted laminar separation. The presence of laminar separation bubbles predicted by the computer program is also indicated in Figure 7. The range of lift coefficient where laminar separation bubbles are present and the chordwise positions predicted are in good agreement with the flow visualization results.

The substantial increase in measured drag compared to calculated drag is due to the disturbance caused by the laminar separation bubble to the starting turbulent boundary layer. A boundary layer trip made up from layers of vinyl tape running spanwise on both top and bottom surfaces at 55% chord produced the drag reduction shown in **Figure 8**. The tape formed a trip 3 mm wide by 0.22 mm high. This was not high enough to cause transition, eliminating the separation bubble entirely, but it did reduce the measured drag.

Drag measurements with the flap extended, shown in Figure 8, also show a substantial reduction in drag, as much as 20%, with boundary layer trips on the top surface of the main wing section.

Bug Tests

Practical wing sections will tend to acquire leading edge roughness due to an accumulation of insect remains even if the wings are carefully maintained and cleaned before flight. The standard NACA sand grain roughness is much too severe to be representative of sailplane wings. Richard H. Johnson[8] has introduced a more reasonable simulation of insect roughness to use in flight tests of sailplanes. Simulated "bugs" made from 5 mm squares of duct tape approximately 0.4 mm thick are attached at the leading edge of intervals of 150 mm and in between each of these on both top and bottom surface 25 mm back from the leading edge to form a pattern of 20 "bugs" per meter. These may not be sufficient to cause immediate transition of the laminar boundary layer, but they certainly will cause some increase in drag. The amount of drag increase is a measure of the sensitivity of the wing section to leading edge roughness.

The result of the bug pattern on drag of this wing section is shown in **Figure 9**. The decrease in drag over part of the operating range will again be due to the effect of these roughness elements on the laminar separation bubble. At higher angles of attack where the laminar boundary layer is not quite so stable there is a large increase in drag due to transition moving forward to give larger coverage of turbulent boundary layer, just the result the "bugs" would be expected to cause.

Comparison With Other Wing Sections

A comparison with wind tunnel test results for the FX67-VC-170/1.36 wing section[9] is shown in **Figure 10**. This wing section was designed by Professor Wortmann specifically for use on the Sigma project. Wing chord can be extended by 36% and at the same time there is a large increase in camber. The comparison shows the FX67-VC-170 is better than the

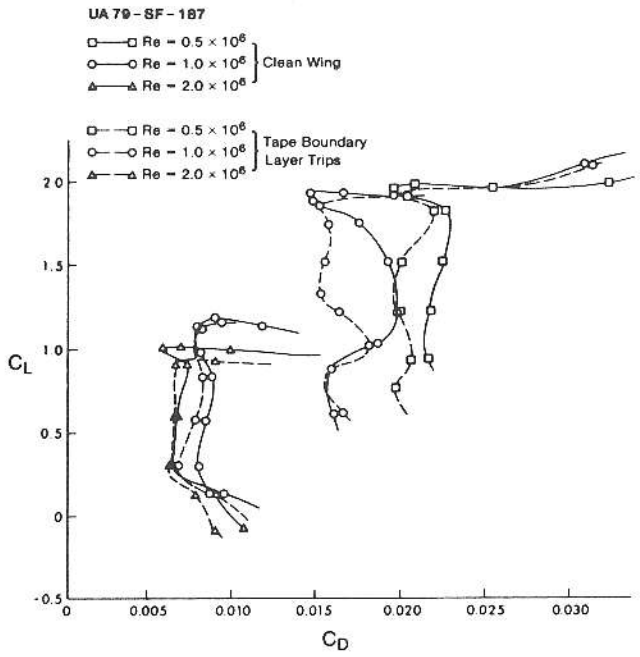

Figure 8. Effect of Boundary Layer Trips on Drag

present design, although performance is very close when the boundary layer trip is used.

The FX67-VC-170/1.36 section appears to have an advantage in that its low drag regime extends to higher lift coefficient with the flap extended. This advantage is more apparent than real, however, since both wing sections have the same C_{Lmax} and both would have to operate at a CL<2 in circling flight to be able to maintain adequate aileron control. The outstanding aileron control power of the slotted flapped wing section will help compensate for its slightly higher drag in a practical application since a more maneuverable aircraft will be better able to center on the lift.

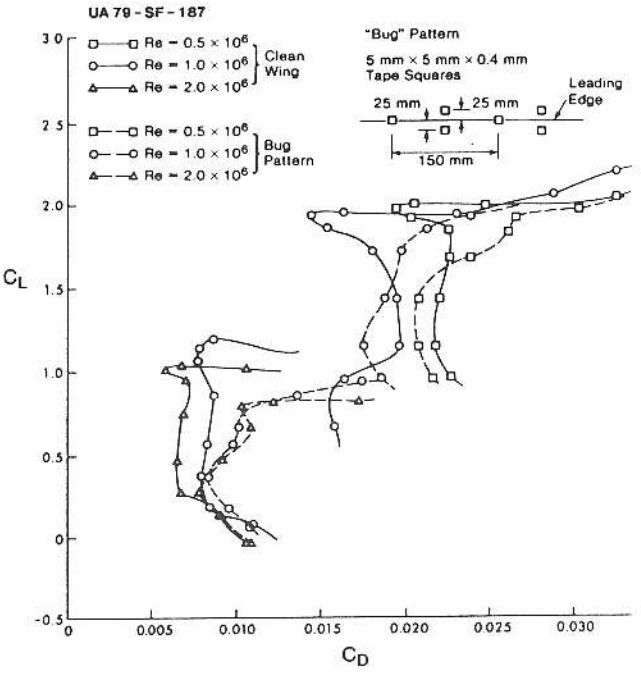

Figure 9. Effect of Leading Edge Roughness

Conclusion

Wind tunnel results for a new slotted flapped wing section are presented, for Reynolds number 1×10^6 and 2×10^6 flap retracted, and 0.5×10^6 and 1×10^6 with flap extended. Lift characteristics are suitable for use on a Variable Geometry Sailplane. Mild stall characteristics in both flap retracted and flap extended configurations will provide docile handling characteristics desirable for safety in any aircraft.

A laminar separation bubble type transition is used to stabilize the extent of laminar flow. This provides low drag over a wide range of lift coefficients. Tests show drag can be reduced by introducing a boundary layer trip just ahead of the laminar separation bubble, even if the trip isn't big enough to eliminate the laminar separation.

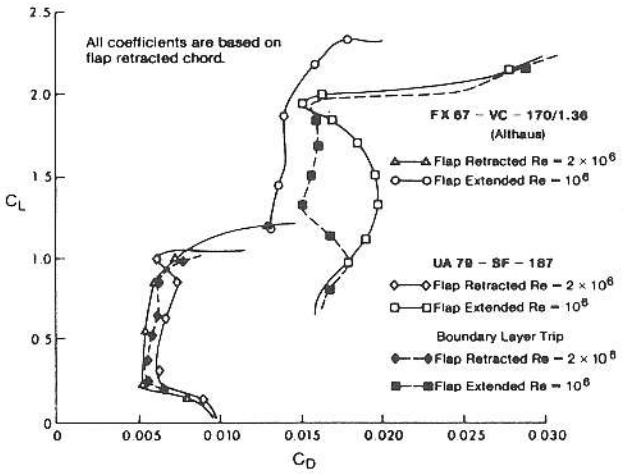

Figure 10. Comparison with FX67-VC-170/1.36

This airfoil should have boundary layer trips for best performance. These could be in the form of pin stripe tape similar to that used to decorate an automobile.

Performance is comparable to the FX76-VC-170/1.36 wing section developed for the Sigma variable geometry sailplane project. The slotted flap type of variable geometry sailplane has practical advantages over the original Sigma concept, and the added thickness, 18.7% compared to 17% will provide structural advantages that may be important for the high aspect ratio wings needed for variable geometry sailplanes.

References

1. Goodhart, N., "Sigma," Sailplane and Gliding, April-May, 1969.

2. Reichmann, H., "New Horizons with an Unconventional Aircraft," Sailplane and Gliding, Nov.-Dec., 1978.

3. Beatty, P. and Johl, F., "The Case for Variable Geometry," Soaring, May, 1968.

4. Marsden, D.J., "Gemini—A Variable Geometry Sailplane," Canadian Aeronautics and Space Journal, Vol. 21, March, 1975.

5. Marsden, D.J., "Prospects For Increased Performance of Sailplanes," Canadian Aeronautics and Space Journal, April, 1971.

6. Kennedy, J. L. and Marsden, D.J., "A Potential Flow Design Method for Multicomponent Airfoil Sections," A.I.A.A. Journal of Aircraft, Vol. 15, January, 1978.

7. Pope, A. and Harper, J.T., "Low Speed Wind Tunnel Testing," John Wiley & Sons Inc.

8. Johnson, R.H., "A Flight Test Evaluation of the Standard Cirrus," Soaring, March, 1976.

9. Althaus, D., Stuttgarter Profilkatalog I Institute fur Aero-und Gasdynamik der Universitat Stuttgart, 1972.